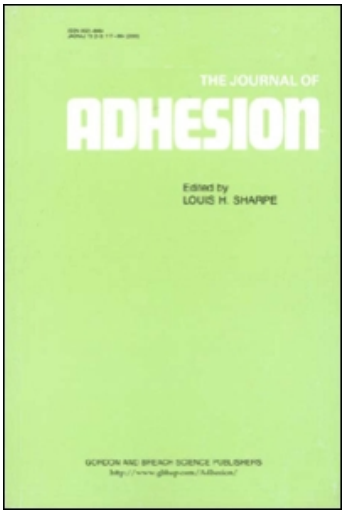

The Journal of Adhesion
Publication details, including instructions for authors and subscription information:
http://www.informaworld.com/smpp/title~content=t713453635

Application of Adhesive Joining Technology for Manufacturing of the Composite Flexspline for a Harmonic Drive

Kwang Seop Jeong[a]; Dai Gil Lee[a]; Yoon Keun Kwak[a]
[a] Department of Precision Engineering and Mechatronics, Korea Advanced Institute of Science and Technology, Taejon-shi, Korea

To cite this Article Jeong, Kwang Seop , Lee, Dai Gil and Kwak, Yoon Keun(1995) 'Application of Adhesive Joining Technology for Manufacturing of the Composite Flexspline for a Harmonic Drive', The Journal of Adhesion, 48: 1, 195 — 216
To link to this Article: DOI: 10.1080/00218469508028162
URL: http://dx.doi.org/10.1080/00218469508028162

J. Adhesion, 1995, Vol. 48, pp. 195–216
Reprints available directly from the publisher
Photocopying permitted by license only

Application of Adhesive Joining Technology for Manufacturing of the Composite Flexspline for a Harmonic Drive

KWANG SEOP JEONG, DAI GIL LEE* and YOON KEUN KWAK

Department of Precision Engineering and Mechatronics, Korea Advanced Institute of Science and Technology, Kusong-dong, Yusong-ku, Taejon-shi, Korea 305-701

(Received January 20, 1994; in final form August 8, 1994)

A new manufacturing method for the cup-type composite flexspline for a harmonic drive was developed using adhesive joining technology to obviate the manufacturing difficulty of the conventional one-piece cup-type steel flexspline and to improve the dynamic characteristics of the flexspline.

In this method, the boss, tube and tooth sections of the flexspline were designed and manufactured separately, and adhesively bonded. The tube section was manufactured with high strength carbon fiber epoxy composite material and its dynamic properties were compared with those of the conventional steel flexspline.

The torque transmission capability of the adhesively-bonded joint was numerically calculated using the nonlinear shear stress-strain relationship which was represented by an exponential form.

From the test results of the manufactured composite flexspline and the conventional steel flexspline, it was found that the manufactured composite flexspline had better torque transmission characteristics. Also, it was found that the damping capacity of the composite flexspline was considerably improved.

KEY WORDS adhesive joining technology; adhesive thickness; adhesive nonlinear property; bonding length; harmonic drive; composite flexspline; torque transmission capability; radial stiffness; dynamic characteristics; damping capacity.

INTRODUCTION

The harmonic drive is a special type of speed reduction mechanism whose principle of operation is based on elastic deformation rather than rigid body motion.[1-3] The harmonic drive is widely accepted in industrial robots and precision mechanisms because of its high speed reduction ratio, high rotational accuracy, high torque transfer per unit of weight, high efficiency and negligible backlash compared with standard gear systems.[4-6]

The harmonic drive is composed of the rigid circular spline, the flexible spline which is called a flexspline and the elliptical wave generator as shown in Figure 1. The ball bearing mounted on the elliptical wave generator deforms the flexspline,

*Corresponding author.

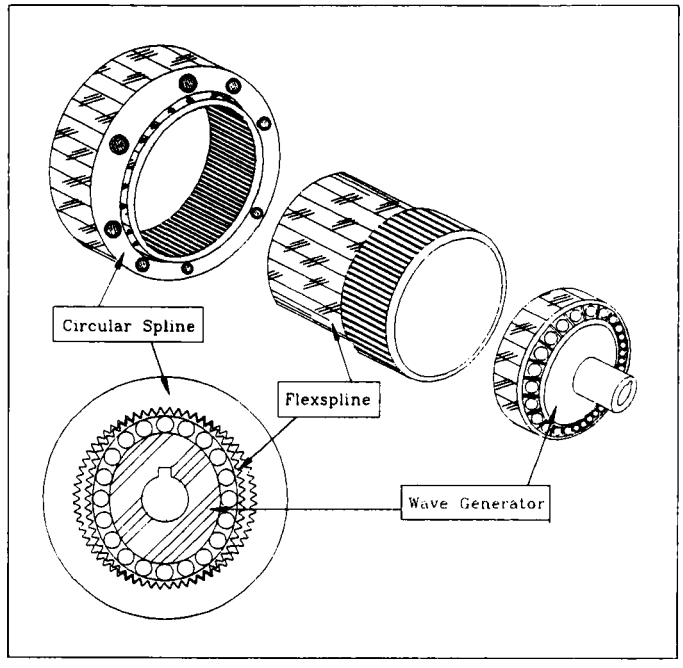

FIGURE 1 Configuration of the cup-type harmonic drive.

thus engaging teeth at diametrically-opposite points coincident with the major axis of the elliptical wave generator and disengaging points at the minor axis. If the rigid circular spline were fixed, then the rotation of the wave generator would produce a reverse motion of the flexspline; if the rigid circular spline has 202 teeth and the flexspline has 200 teeth, then the single revolution of the wave generator will rotate the flexspline backward two teeth. In this case, the rotational velocity ratio would be 100:1. The number of teeth of the flexspline is usually two or four less than the number of the circular spline.

The input torque of the harmonic drive is usually applied to the shaft of the wave generator which is pressure fitted to the open end of the flexspline and the output torque is applied to the shaft at the close end of the flexspline. Therefore, the flexspline is the most important part of the harmonic drive and determines the performance of the harmonic drive.

The flexspline of the harmonic drive has usually the one-piece cup-type shape as shown in Figure 2.[7]

The manufacture of the cup-type flexspline of Figure 2 usually requires a boring operation of a solid cylinder and special jigs to hob teeth, which requires much machining time and large material loss.

Even though the harmonic drive has many kinematic advantages, it has several dynamic drawbacks; the motion is not perfectly smooth but has a ripple which has the same frequency as the wave generator.[8] The ripple can produce noise or vibra-

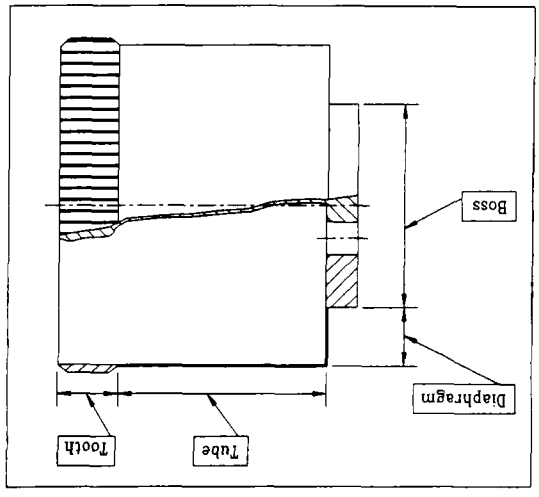

FIGURE 2 Shape of the cup-type flexspline.

tion when the natural frequency of the flexspline becomes the same as the exciting frequency. Also, the torsional stiffness of the flexspline is small and decreases as the torque increases because it is designed as a thin cup shape to decrease the radial stiffness.[8] These phenomena can not be avoided when the flexspline is made of conventional isotropic materials such as steel and aluminum.

If a carbon fiber epoxy composite material which has high specific stiffness,[9] high specific strength and high damping capacity is used as the material for the flexspline, the torsional stiffness can be increased independently of the radial stiffness by adjusting the stacking angle of the composite material. Also, since many high strength adhesives have been developed,[10] adhesive joining of separately-manufactured composite and steel parts has been possible.

There has been an attempt to manufacture the flexspline using adhesive joining of separately-manufactured parts.[11] Figure 3 shows the shape of the flexspline manufactured by the method, in which the steel tooth section was adhesively-joined to the machined surface of the composite tube. In this method, the thickness of the root tube under the steel tooth should be small to make the radial stiffness of the flexspline small. Also, the fiber breakage of the composite tube in machining was inevitable. Consequently, it was found that the tooth was failed by fatigue in continuous prolonged operation.

Therefore, a new manufacturing method for the composite flexspline which can obviate the fatigue problem of the steel tooth section was developed. The one-piece, cup-type flexspline was divided into three parts such as the boss, tube and tooth sections. This method eliminated machining of the surface of the composite tube on which the steel tooth section was adhesively-bonded. Since the thickness of the root tube of the tooth section can be increased without increasing the radial stiffness in this method, the possibility of fatigue failure in the tooth section was decreased.

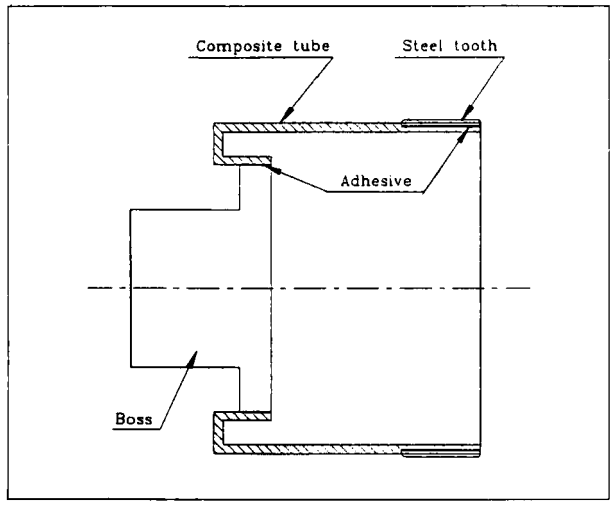

FIGURE 3 Sectional shape of the composite flexspline.

The boss and tooth sections were made of S45C steel and the tube section was made of high strength carbon fiber epoxy composite material. The conventional one-piece, cup-type flexspline was also manufactured with S45C steel in order to compare the performances.

Since the nonlinear adhesive properties must be included in order to calculate accurately the torque capacity of the adhesive joint, in this paper the shear stress-strain curve was represented in an exponential form using two parameters such as the initial shear modulus and the ultimate shear strength and was used in numerical calculation.

The static and dynamic characteristics such as the torque transmission capability, radial and torsional stiffnesses, natural frequency and damping capacity were measured and compared with those of the one-piece, cup-type steel flexspline. From the experimental results, it was found that the developed composite flexspline had sufficient torque transmission capability, its initial torsional stiffness was improved more than 50% and the damping capacity at the fundamental natural frequency was improved more than 100%.

DESIGN AND MANUFACTURE OF THE COMPOSITE FLEXSPLINE

In this work, a harmonic drive which has the average maximum torque of 100 N·m and the instant maximum torque of 150 N·m, was selected. Figure 4 shows the specifications of the one-piece, cup-type flexspline which has the required transmission capabilities.

Figure 5 shows the manufacturing scheme for the adhesively-bonded composite flexspline. The flexspline of Figure 4 was divided into three parts as shown in Figure 5a and was adhesively-bonded as shown in Figure 5b.

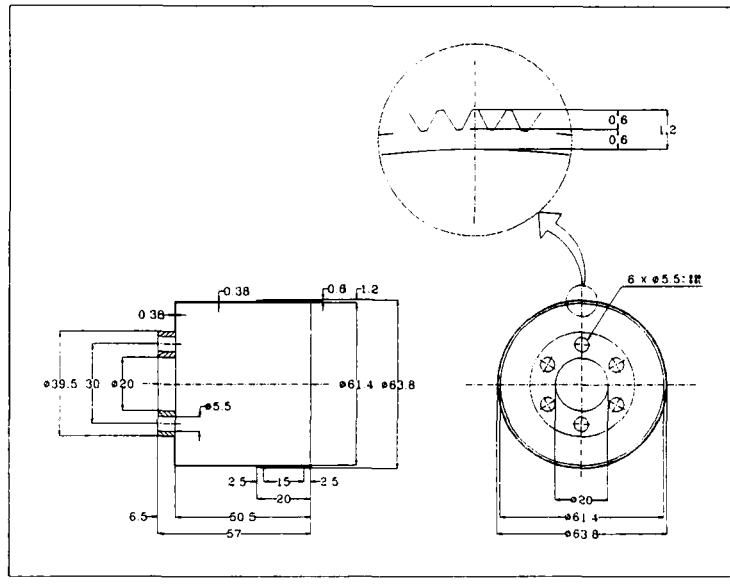

FIGURE 4 Dimensions of the manufactured cup-type steel flexspline.

Two bonding methods may be applied in joining the three parts of the flexspline as shown in Figure 6. Figure 6a shows the bonding method in which the composite tube is adhesively-bonded to the inside surface of the steel tooth, while, in Figure 6b, the composite tube is adhesively bonded to the outside surface of the steel tooth. Since the torsional stiffness and torque transmission capability of the adhesively-bonded joint increases as the average radius of the adhesive area increases, in this work the outside bonding as shown in Figure 6b was selected.

Since the buckling failure, as well as the shear failure, is important for the thin-walled torsional composite tube, the critical torsional buckling torque and the maximum shear torsional shear stress were calculated using the previous research results. The maximum torsional shear stress τ_{max} was expressed by Eq. (1).[12]

$$\tau_{max} = \frac{T_{max}}{2\pi r^2 t} \tag{1}$$

where T_{max} is the applied maximum torque, r is the mean radius and t is the thickness of the tube.

The critical buckling torque T_{cr} was expressed by Eq. (2).[13]

$$T_{cr} = 24.4(C)(D_{22})^{5/8}(A_{11})^{3/8}(r_a)^{5/4}(L)^{-1/2} \tag{2}$$

where, L is the tube length, A_{11} the extentional stiffness, D_{22} the bending stiffness, and C is the end-fixity coefficient which is 0.925 for the simply-supported and 1.03 for the clamped end.

Since the torque transmission characteristics of the flexspline is most important, the stacking sequences $[\pm 45]_{nS}$ or $[\pm 45]_{nT}$ should be employed to make shear

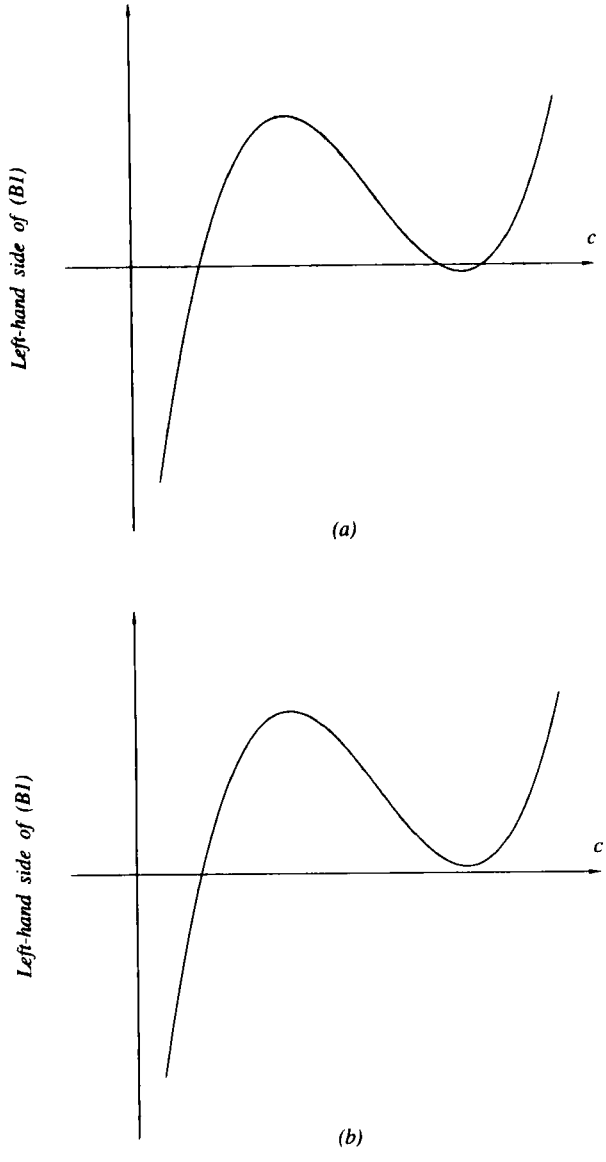

FIGURE 5 Shapes of the developed composite flexspline: a) three parts and b) assembled shape.

properties maximum.[14,15] The subscripts n, S and T represent the number of plies, symmetry and totality of plies, respectively. If the prepreg is laid-up in the symmetric mode, there exists a seam between prepreg plies. Therefore, the stacking sequence $[\pm 45]_{nT}$, which does not have fiber discontinuity, was employed in this work.

The high strength carbon fiber epoxy prepreg, which was manufactured by Sunkyong Fiber Co.,[16] was hand laid-up and cured by an autoclave vaccum bag

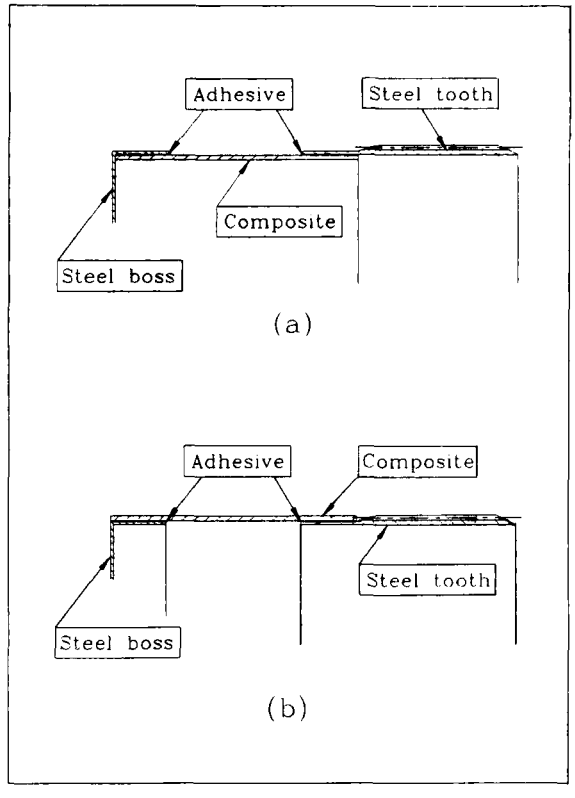

FIGURE 6 Bonding of the composite tube to the steel tooth: a) inside bonding and b) outside bonding.

degassing molding process. The tensile property of the undirectional composite was determined by ASTM D 3039-76 and the shear property was determined by ASTM D 3518-76. Table I shows the measured properties of the carbon fiber epoxy composite material.

TABLE I
Mechanical properties of the USN 150 uni-directional carbon fiber epoxy composite by ASTM 3039-76

Tensile modulus	0°(E_L)	130 GPa
	90° (E_T)	8 GPa
Shear modulus (G_{LT})		6 GPa
Tensile strength	0°(X)	1,800 MPa
	90°(Y)	60 MPa
Shear strength (S)		75 MPa
Poisson's ratio (ν_{LT})		0.28
Thickness per ply		0.15 mm

The properties of the composite laminate whose stacking sequence was $[\pm 45]_{nT}$ was calculated by the classical laminated plate theory[17] as shown in Table II.

The adhesive material used was HYSOL EA 9309.2 NA.[18] The tensile property of the adhesive was determined by ASTM D 638-89, the shear property was determined by ASTM D 3518-76 and the lap shear strength was determined by ASTM D 1002-72. Table III shows the measured properties.

Since the inner diameter of the composite tube is the sum of the outside diameter of the boss section and twice the adhesive thickness, the adhesive thickness must be determined first in order to determine the dimensions of the composite tube.

The adhesive thickness affects the torsional strength of adhesively-bonded tubular lap joints. Even though there have been many investigations on adhesively bonded tubular lap joints,[19–21] the real dynamic characteristics of adhesively-bonded tubular lap joints have seldom been accurately predicted because they are dependent on the surface roughness of the adherend, humidity, cure condition and the bonding skill of personnel. Since a research result on the fatigue strength of the adhesively bonded tubular single lap joint suggested, the use 0.1 mm adhesive thickness,[22] this value was chosen.

In order to determine the thickness of the composite tube, Eq. (1) was changed to the following form:

$$\tau_{\max} = \frac{T_{\max}}{2\pi r^2 t} = \frac{2T_{\max}}{\pi(D_i + t)^2 t} = \frac{2T_{\max}}{\pi D_i^2 t + 2\pi D_i t^2 + \pi t^3} \tag{3}$$

where D_i is the inner radius of the tube.

The shear strength, $\tau_{\max}$, of the composite material with stacking sequence $[\pm 45]_{nT}$ was 445 MPa, which was measured by ASTM D 4255-83. When four plies

TABLE II
Mechanical properties of the $[\pm 45]_{nT}$ laminated composites

Longitudinal elastic modulus (E_1)	20.55 GPa
Transverse elastic modulus (E_2)	20.55 GPa
Longitudinal transverse Shear modulus (G_{12})	33.54 GPa
Poisson's ratio (ν_{12})	0.712

TABLE III
Properties of the HYSOL EA 9309.2 NA adhesive

Mixing ratio by weight (Resin:Hardener)	100:22
Minimum curing time	7 day (at 25°C) 1 hour (at 75°C)
Mixed viscosity	1,500 Poise
Service temperature	80°C
Tensile modulus	1.43 GPa (at 25°C)
Shear modulus	0.51 GPa (at 25°C)
Tensile strength	42.0 MPa (at 25°C)
Lap shear strength	14.2 MPa (at 25°C)
Lap shear strain limit	0.11
Poisson's ratio	0.40

were stacked, the thickness of the composite tube was 0.6 mm and the inner radius of the composite tube was 62.4 mm. Then, the shear stress of the tube when the maximum instantaneous torque 150 N·m was applied, was 40.1 MPa from Eq. (3). Since the safety factor was 11.1 in this case, this value of composite thickness was selected.

In order to determine the bonding length for the composite flexspline, the nonlinear adhesive properties must be included because the majority of the load transfer of the adhesively-bonded joint is accomplished by the nonlinear elastic behavior of the adhesive.

Several researchers included the nonlinear adhesive properties in their analyses through stress-strain curves composed of two parts: linear elastic and nonlinear plastic.[23] The two-part representation of the stress-strain behavior requires the elastic strain limit and the magnitude of the strain must be compared with the elastic strain limit in numerical calculation.

Therefore, in this paper, the shear stress, τ_a, *versus* shear strain, γ_a, curve of the adhesive was represented by one curve using two parameters, the initial shear modulus, G_a, and the ultimate shear strength, τ_m, as follows.

$$\tau_a = \tau_m \cdot (1 - e^{-G_a/\tau_m \cdot \gamma_a}) \tag{4}$$

Figure 7 shows both the experimental shear stress-strain curve and the Eq. (4) for HYSOL EA 9309.2 adhesive. Table III shows the properties of the adhesive. From Figure 7, it was found that Eq. (4) could represent the experimental data with less than 7% error, which was a better representation than the linear elastic-plastic curve.

For the adhesive single lap joint, as shown in Figure 8, the relationship between the torque, T_s in the steel adherend, the torque, T_c, in the composite adherend and the applied torque, T, can be represented by the following equation.[24]

$$T = T_s + T_c = \frac{\tau^s_{z\theta} \cdot J_s}{r_1} + \frac{\tau^c_{z\theta} \cdot J_c}{r_2} = \text{constant} \tag{5}$$

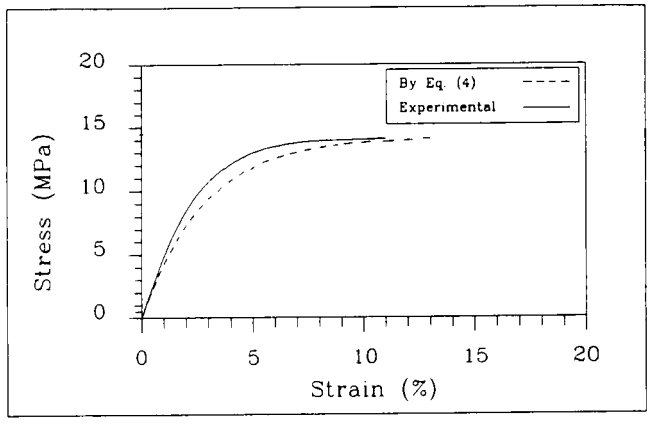

FIGURE 7 Shear stress-strain curve of the epoxy adhesive (HYSOL EA 9309.2).

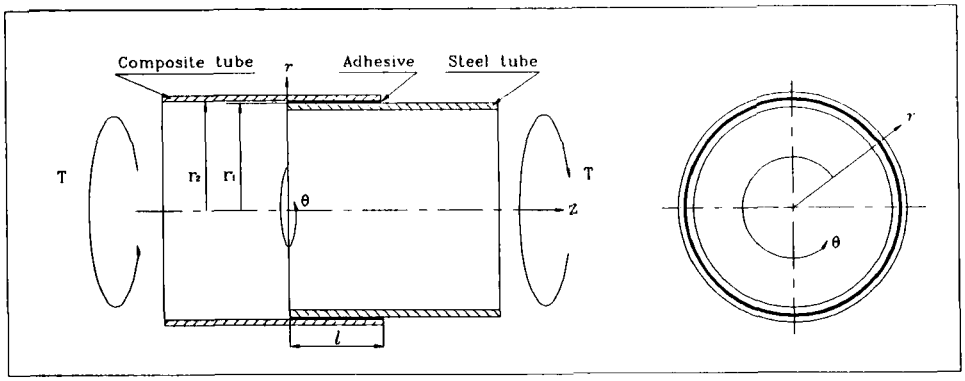

FIGURE 8 Configuration of the adhesively bonded tubular single lap joint.

where, $\tau^s_{z\theta}$ is the shear stress of the steel tube at r_1, $\tau^c_{z\theta}$ the shear stress of the composite tube at r_2, J_s the sectional polar moment of inertia of the steel tube, and J_c the sectional polar moment of inertia of the composites tube.

Assuming that the adhesive is an isotropic material and the thickness of the adhesive is small, the variations of the torque in z-direction are expressed as follows.

$$\frac{dT_c}{dz} = -2\pi \cdot r_a^2 \cdot \tau_a \tag{6}$$

$$\frac{dT_s}{dz} = 2\pi \cdot r_a^2 \cdot \tau_a \tag{7}$$

where, $r_a = (r_1 + r_2/2)$ is the average radius of the adhesive.

The geometric compatibility between the shear strain of the adhesive and the shear strains of the adherends can be written as follows.

$$\begin{aligned}\frac{d\gamma_a}{dz} &= \frac{\gamma^s_{z\theta} - \gamma^c_{z\theta}}{t_a} = \frac{1}{t_a}\left(\frac{T_s \cdot r_1}{G^s_{z\theta} \cdot J_s} - \frac{T_c \cdot r_2}{G^c_{z\theta} \cdot J_c}\right) \\ &= \frac{1}{t_a}\left\{\frac{T \cdot r_1}{G^s_{z\theta} \cdot J_s} - \left(\frac{r_1}{G^s_{z\theta} \cdot J_s} + \frac{r_2}{G^c_{z\theta} \cdot J_c}\right) \cdot T_c\right\}\end{aligned} \tag{8}$$

where $\gamma^c_{z\theta}$ is the shear strain of the composite tube at r_2, $\gamma^s_{z\theta}$ the shear strain of the steel tube at r_1, $t_a (= r_2 - r_1)$ the thickness of the adhesive and $G^c_{z\theta}$, $G^s_{z\theta}$ the shear moduli of the composite tube and the steel tube, respectively.

Differentiating Eq. (8) with respect to z, the following equation is obtained.

$$\frac{d^2\gamma_a}{dz^2} = -\frac{1}{t_a}\left(\frac{r_1}{G^s_{z\theta} \cdot J_s} + \frac{r_2}{G^c_{z\theta} \cdot J_c}\right) \cdot \frac{dT_c}{dz} \tag{9}$$

Combining Eqs. (4), (6) and (10), the governing differential equation of the shear strain of the adhesive was obtained as follows.

$$\begin{aligned}\frac{d^2\gamma_a}{dz^2} &= \frac{2\pi \cdot r_a^2}{t_a} \cdot \left(\frac{r_1}{G^s_{z\theta} \cdot J_s} + \frac{r_2}{G^c_{z\theta} \cdot J_c}\right) \cdot \tau_m \cdot (1 - e^{-G_a/\tau_m \cdot \gamma_a}) \\ &= \delta \cdot \tau_m \cdot (1 - e^{-G_a/\tau_m \cdot \gamma_a})\end{aligned} \tag{10}$$

where,

$$\delta = \frac{2\pi \cdot r_a^2}{t_a} \cdot \left(\frac{r_1}{G_{z\theta}^s \cdot J_s} + \frac{r_2}{G_{z\theta}^c \cdot J_c} \right) \tag{11}$$

The boundary conditions for Eq. (11) are as follows.
When $z = 0$, $T_c = T$, $T_s = 0$

$$\left. \frac{d\gamma_a}{dz} \right]_{z=0} = \gamma'_a(0) = -\frac{1}{t_a} \cdot \left(\frac{T \cdot r_2}{G_{z\theta}^c \cdot J_c} \right) \tag{12}$$

$$\left. \frac{d^2\gamma_a}{dz^2} \right]_{z=0} = \gamma''_a(0) = \delta \cdot \tau_m \cdot (1 - e^{-G_a/\tau_m \cdot \gamma_a(0)}) \tag{13}$$

$$\left. \frac{d^3\gamma_a}{dz^3} \right]_{z=0} = \gamma'''_a(0) = \delta \cdot G_a \cdot (e^{-G_a/\tau_m \cdot \gamma_a(0)}) \cdot \gamma'_a(0) \tag{14}$$

When $z = l$, $T_c = 0$, $T_s = T$

$$\left. \frac{d\gamma_a}{dz} \right]_{z=l} = \gamma'_a(l) = \frac{1}{t_a} \cdot \left(\frac{T \cdot r_1}{G_{z\theta}^s \cdot J_s} \right) \tag{15}$$

Equation (10) was solved numerically[25] by using the Taylor series expansion method as follows.

$$\gamma_a(z+h) = \gamma_a(z) + \gamma'_a(z) \cdot h + \gamma''_a(z) \cdot \frac{h^2}{2} + \gamma'''_a(z) \cdot \frac{h^3}{6} + \cdots \tag{16}$$

$$\gamma'_a(z+h) = \gamma'_a(z) + \gamma''_a(z) \cdot h + \gamma'''_a(z) \cdot \frac{h^2}{2} + \cdots \tag{17}$$

$$\gamma''_a(z+h) = \gamma''_a(z) + \gamma'''_a(z) \cdot h + \cdots \tag{18}$$

$$\gamma'''_a(z+h) = \gamma'''_a(z) + \cdots \tag{19}$$

where $\gamma_a(z)$ is the shear strain at distance z and h is the incremental distance along the z-axis.

The maximum torque capacity can be calculated by assuming that either end of the adhesive reaches the failure shear strain γ_f. Since the first derivative of the shear strain γ'_a becomes smaller as the shear strain approaches the failure strain, which end will reach the failure strain first can be determined by comparing $|\gamma'_a(0)|$ and $|\gamma'_a(l)|$. Then the other end should satisfy the condition of the first derivative of the shear strain. In this work, the first adhesive failure occured at $z = 0$. Since the first derivative contains the applied torque, T, this condition gives the maximum torque. In the numerical calculation, the first trial value of T was calculated by assuming that all the adhesive reaches the ultimate shear stress, τ_m, and then the value of torque was decreased successively to satisfy the first derivative of the boundary conditions.

Table IV shows the data for the adhesively-bonded single lap joint used to manufacture the composite flexspline. In Table IV, the steel and composite tube were assumed to be isotropic and orthotropic materials, respectively.

Figure 9 shows the maximum torque transmission capability of the adhesive joint of Figure 8 with respect to the bonding length when the data in Table IV were used.

TABLE IV
Data of the adhesively-bonded single lap joint used to manufacture the composite flexspline

	HYSOL EA 9309.2 NA	Steel tube (S45C)	Composite tube $[\pm 45]_{2T}$
Shear modulus (GPa)	0.51	80	33.54
Shear strength (MPa)	14.2	not required	not required
Shear strain limit	0.11	not required	not required
Thickness (mm)	0.1	0.38	0.6
Inner radius (mm)		30.7	31.4
Outer radius (mm)		31.08	32.0

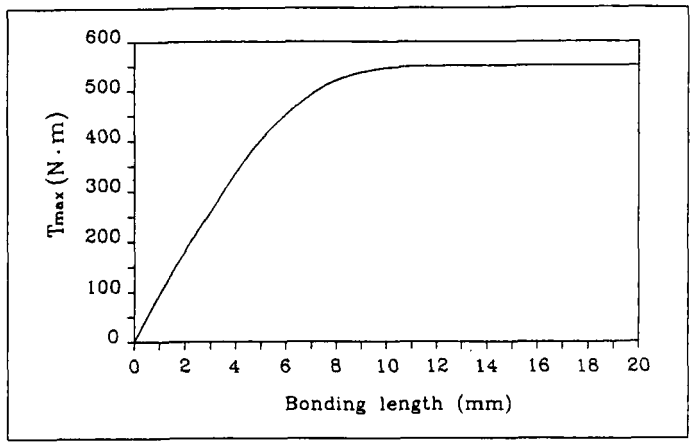

FIGURE 9 Effect of the bonding length on the maximum static torque transmission capability.

Since the maximum torque became saturated when the bonding length was larger than about 10 mm, a 7 mm bonding length was chosen. Figure 10 shows the shear strain and shear stress distributions in the adhesive when the bonding length is 7 mm and the maximum static torque is 490 N·m. Since the required torque of the designed harmonic drive is 150 N·m, it was found that a 7 mm bonding length is enough for the torque capacity.

Figure 11 shows the shear strain and shear stress distributions in the adhesive when the bonding length is 7 mm and the applied torque is 150 N·m.

From Figure 11, it was found that the shear stresses at $z = 0$ and $z = l$ were 7.6 MPa and 6.2 Mpa, respectively, which were less than the adhesive shear strength, 14.2 MPa. Then, the total length of the composite tube was determined to be 30.88 mm.

Figure 12 shows the final dimensions of the composite flexspline.

In order to check the buckling failure of the designed composite tube using Eq. (2), the values of A_{11} and D_{22} were determined using classical lamination plate theory, as follows.

$$A_{11} = 21.52\,\text{MN/m}$$

$$D_{22} = 0.485\,\text{N·m}$$

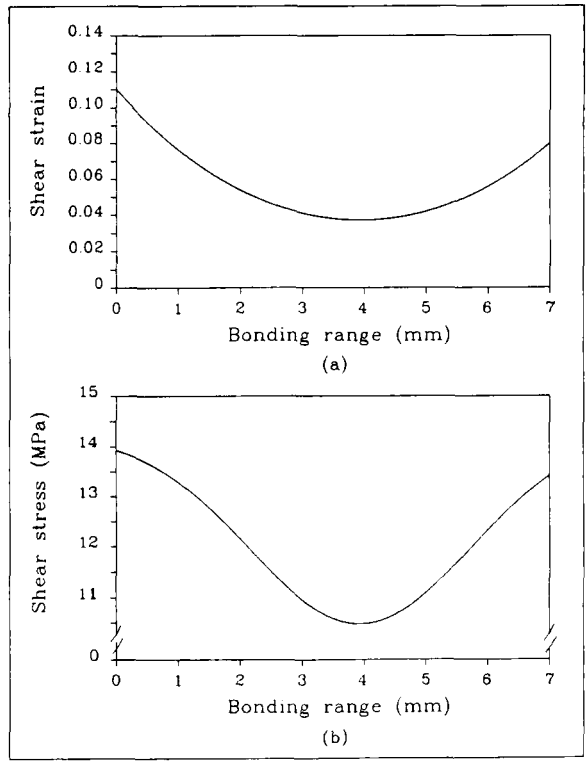

FIGURE 10 Shear strain and stress distributions in the adhesive when the bonding length is 7 mm and $T_{max} = 490\,N \cdot m$ is applied to the joint: a) shear strain and b) shear stress.

Since the input and output shafts of the flexspline are usally simply-supported by ball bearings, the end fixity constant C was selected to be 0.925.

Using these values, the critical buckling torque was calculated to be $610\,N \cdot m$. Since the safety factor for the buckling torque was over 4.0, the designed flexspline was satisfactory. With the specifications determined so far, the adhesively-bonded composite flexspline was manufactured.

Figure 13a shows the separately-manufactured boss, composite tube and tooth section. Figure 13b shows the assembled composite flexspline using adhesive bonding technology. Figure 13c shows the conventional S45C steel one-piece flexspline.

In the adhesive bonding of the three parts of the composite flexspline, the jig as shown in Figure 14 was used for the concentric bonding operation.

EXPERIMENTS AND DISCUSSIONS

The static torque transmission capability of the adhesively-bonded composite flexspline was compared with that of the conventional one-piece S45C steel flexspline. In order to give the flexspline the same conditions as induced in the assembled state

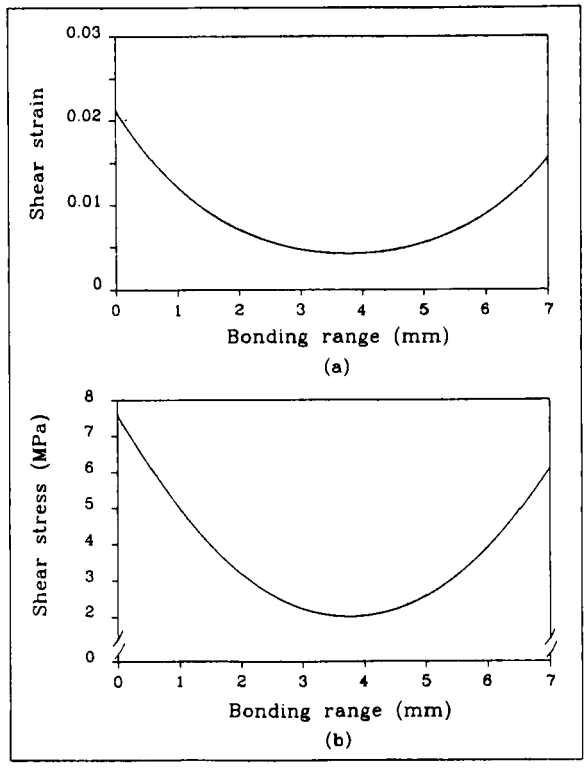

FIGURE 11 Shear strain and stress distributions in the adhesive when the bonding length is 7 mm and $T = 150\,\text{N}\cdot\text{m}$ is applied to the joint: a) shear strain and b) shear stress.

with the wave generator, the elliptic jig as shown in Figure 15 was manufactured and used in the tests of torque transmission capability.

Figure 16 shows the static torque transmission capabilities of the adhesively-bonded composite flexspline and the conventional S45C steel flexspline. The torque transmission capabilities were measured with the multi-axial material testing system MTS 319.10.[26]

In the torque transmission tests, the adhesively-bonded composite flexspline failed at the adhesively-bonded area between the composite tube and the tooth section, while the S45C steel flexspline failed at the edge between the tube and the flange as shown in Figure 17. Since the torque transmission capability of the adhesively-bonded composite flexspline was more than $475\,\text{N}\cdot\text{m}$, it was concluded that the developed flexspline had enough torque transmission capability compared with the required maximum average and maximum instantaneous torque transmission capabilities, and that the developed calculation method for torque capacity using the nonlinear shear stress-strain gave a fairly accurate estimation, with an error less than 5%.

The torsional stiffness of the harmonic drive is defined as the ratio of the applied torque to the twisting angle. The initial stiffness of the harmonic drive, which is

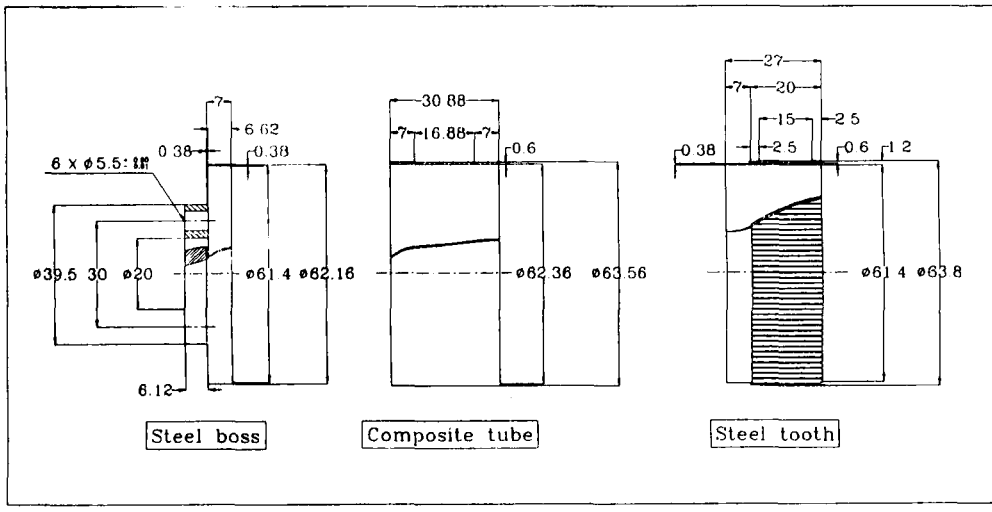

FIGURE 12 Dimensions of the developed composite flexspline.

measured at a torque less than one-half of the rated capacity, is important when it is employed as a precision servo drive mechanism. Therefore, the stiffness of the harmonic drive is usually determined near the initial slope.[27]

Figure 18a shows the method of stiffness determination. The initial stiffness, K_1, is determined in the range of 0 to 10% of the average maximum torque, the intermediate stiffness, K_2, in the range of 10 to 50% of the average maximum torque and the maximum stiffness, K_3, in the range of 50% to the maximum torque. From Figure 18a, K_1 and K_2 are important for a precise servo drive mechanism. Figure 18b shows the stiffness of the adhesively-bonded composite flexspline and Figure 18c shows the stiffness of the conventional S45C steel flexspline. In Figure 18, the applied torques T_1 and T_2 were $10\,N$ and $50\,N$, respectively. The testing system used was the MTS 319.10.

From the experimental results of Figure 18, it was found that the stiffnesses K_1 and K_2 were increased 53% and 22%, respectively, compared with those of the S45C steel flexspline.

In order to measure the radial stiffness of the flexspline, the stiffness measuring device shown in Figure 19 was manufactured.

In the measurement of the radial stiffness, weights on the flexspline were increased and corresponding displacements were measured after a reference initial displacement was defined with a gauge block. When the applied weight on the flexspline was $40\,N$, the radial displacements of the composite flexspline and the steel flexspline were 693 μm and 679 μm, respectively. In this case, the radial compliances of the composite flexspline and the steel flexspline were $17.32\,\mu m/N$ and $16.97\,\mu m/N$, respectively. Accordingly, it was found that the radial compliance of the composite flexspline was increased about 2% compared with that of the steel flexspline.

The vibrational characteristics of the flexspline were measured by the impulse-frequency response. The apparatus for measurement was a dual channel fast Fourier

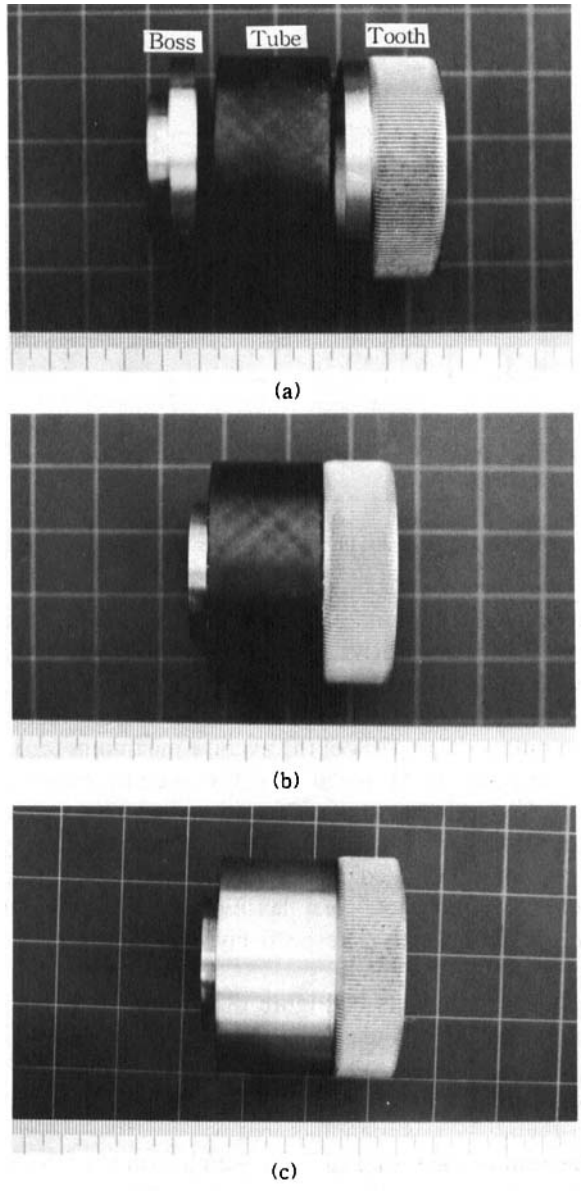

FIGURE 13 Manufactured flexsplines: a) boss, tube and tooth sections, b) assembled composite flexspline and c) one-piece steel flexspline. See Color Plate I.

transform analyzer (B&K 2032), a charge amplifier (B&K 2635), an impulse hammer (B&K 8202), an accelerometer (B&K 4374), a force transducer (B&K 8200), and a personal computer for data acquisition. Two impulses were given to the flexspline in both the radial and torsional directions as shown in Figure 20.

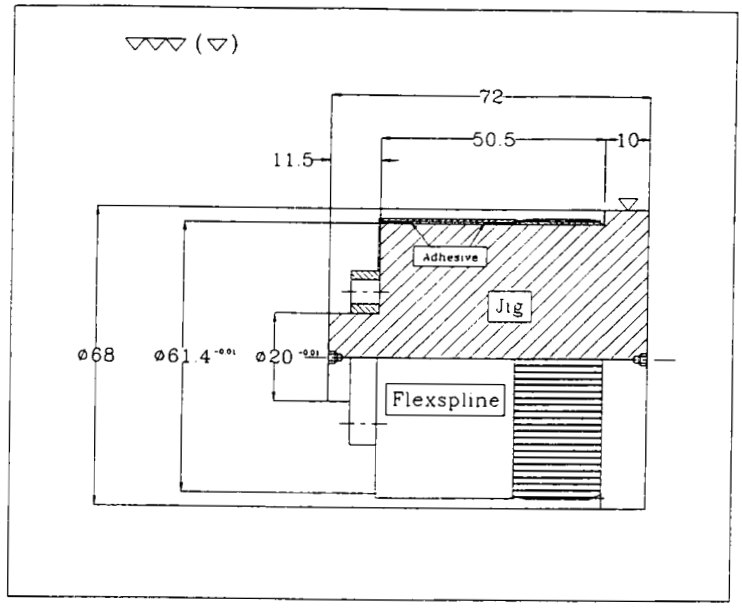

FIGURE 14 Configuration of the adhesvie bonding assembly.

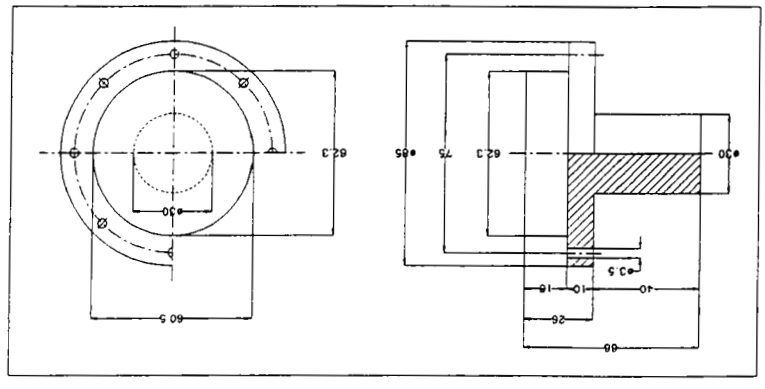

FIGURE 15 Elliptic jig shape for the static torque transmission capability test.

Figure 20a shows the measurement in the radial direction and Figure 20b shows the measurement in the torsional direction. In order to measure the torsional vibration characteristics of the flexspline, a small steel tip for accelerometer mounting adhesively-bonded as shown in Figure 20b and an impulse was given to the opposite position of the accelerometer.

Table V shows the experimental results.

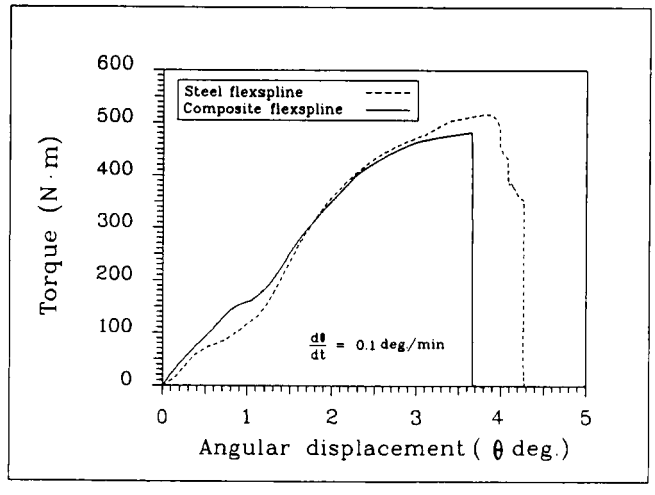

FIGURE 16 Static torque transmission capabilities of the flexsplines.

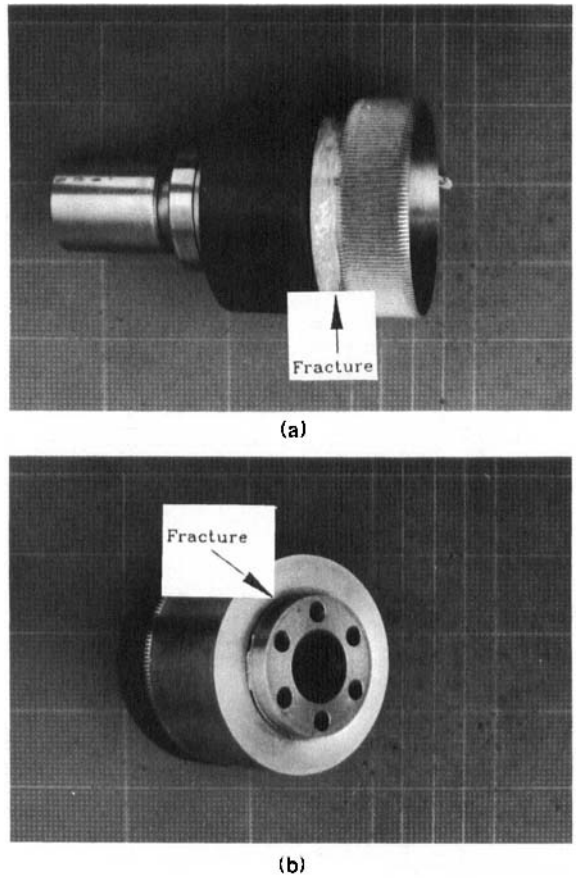

FIGURE 17 Fracture sites of the flexsplines: a) composite flexspline and b) steel felxspline. See Color Plate II.

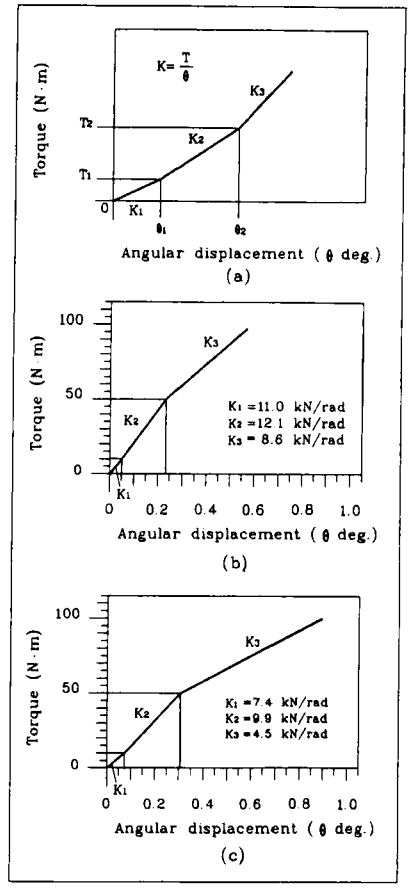

FIGURE 18 Torque-twisting angle curves for determination of circulation direction stiffness: a) general type, b) composite flexspline and c) steel flexspline.

TABLE V
Fundamental natural frequencies and damping ratios

	Mode	Frequency (Hz)	Damping ratio (ζ)
Composite flexspline	Radial	475.0	0.00351
	Twisting	396.5	0.00432
Steel flexspline	Radial	416.5	0.00171
	Twisting	368.5	0.00147

From Table V, it was found that the fundamental natural frequency and damping of the adhesively-bonded composite flexspline were increased 14% and 105%, respectively, in the radial direction, and 7.5% and 190%, respectively, in the torsional direction, compared with those of the S45C steel flexspline.

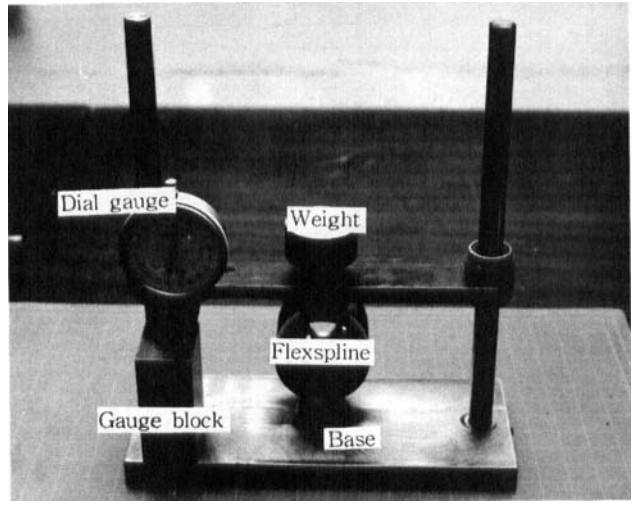

FIGURE 19 Measurement of the radial stiffiness of the flexspline. See Color Plate III.

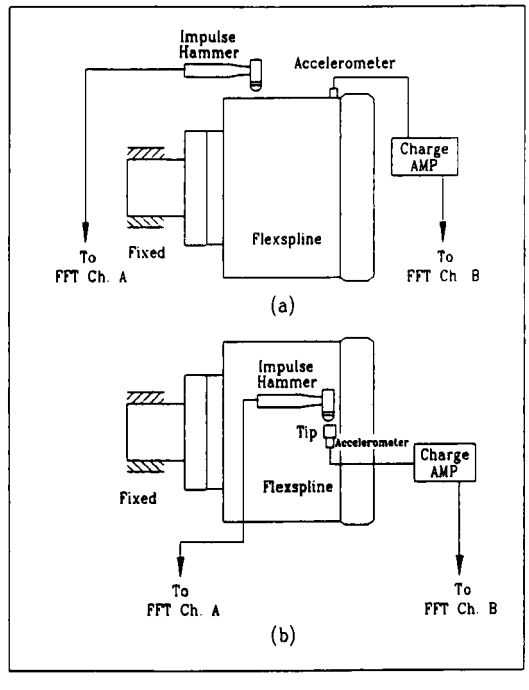

FIGURE 20 Experimental setup for the impulse – frequency response test: a) radial vibration and b) torsional vibration.

CONCLUSIONS

In this work, a new manufacturing method for the cup-type composite flexspline for a harmonic drive was developed using adhesive joining technology to obviate the manufacturing difficulty of the conventional one-piece, cup-type steel flexspline and to improve the dynamic characteristics of the flexspline. The boss, tube and tooth sections of the flexspline were manufactured separately, and adhesively bonded. The boss and tooth sections were made of S45C steel and the tube section was manufactured with high-strength carbon fiber epoxy composite material. The torque transmission capability of the adhesively-bonded joint of the flexspline, was numerically calculated using a nonlinear adhesive shear stress-strain model.

The static and dynamic characteristics such as the torque transmission capability, radial and torsional stiffnesses, natural frequency and damping capacity of the adhesively-bonded composite flexspline were measured and compared with those of the conventional one-piece, cup-type steel flexspline. From the experimental investigation, the following conclusions were made:

(1) The adhesively-bonded composite flexspline had enough torque transmission capability.
(2) The nonlinear shear stress-strain model was adequate for the calculation of the properties of the adhesively-bonded joint design.
(3) The torsional stiffnesses of the adhesively-bonded composite flexspline were increased more 50 and 20% in the initial and intermediate torque ranges, respectively, compared with those of the conventional one-piece S45C steel flexspline.
(4) The radial compliance of the adhesively-bonded composite flexspline was increased 2% compared with that of the steel flexspline.
(5) The natural frequencies at the radial and torsional modes were increased 14% and 7.5%, respectively, compared with those of the conventional one-piece S45C steel flexspline.
(6) The damping capacities in the radial and torsional modes were increased 105% and 190%, respectively, compared with those of the conventional one-piece S45C steel flexspline.

References

1. C. W. Musser, "Strain wave gearing," United States Patent, No. 2,906,143, Sept. 29, 1959.
2. C. W. Musser, "Breakthrough in mechanical drive design: The harmonic drive," *Machine Design*, April 14, 160–173 (1960).
3. C. W. Musser, "A new look at elastic-body mechanics," *Machine Design*, April 13, 160–173 (1961).
4. C. Nicholas, "Innovation in high-ratio gearing," *Product Engineering*, February 8, 47–51 (1960).
5. J. H. Carlson, "Harmonic drive for servomechanisms," *Machine Design*, January 6, 102–106 (1985).
6. L. Giovanni and F. Rodolfo, "Harmonic drive transmissions: the effects of their elasticity, clearance and irregularity on the dynamic behaviour of an actual SCARA robot," *Robotica* **10**, 369–375 (1992).
7. Y. Kiyosawa and M. Sasahara, "Development of a new thin harmonic drive," *JSME*, Robotics and mechatronics lecture meeting paper, A, 943–948 (1992).
8. G. B. Andeen (Edition), *Robot Design Handbook* (McGraw-Hill, New York, 1988), Chap. 11.
9. R. M. Jones, *Mechanics of Composite Materials* (Scripta Book Co., Washington, D. C., 1975), Chap. 1.
10. A. J. Kinloch, *Adhesion and Adhesives* (Chapman and Hall, New York, 1987), Chap. 1.
11. H. S. Oh, K. S. Jeong and D. G. Lee, "Design and manufacture of the composite flexspline of a harmonic drive with adhesive joining", *Composite Structures*, **28**, 307–314 (1994).

12. J. M. Whitney and J. C. Halpin, "Analysis of laminated anisotropic tubes under combined loading," *J. Composite Mater.* **2**, 360–372 (1968).
13. G. J. Simitses, "Instability of orthotropic cylindrical shells under combined torsion and hydrostatic pressure," *AIAA Journal* **5**, 1463–1475 (1967).
14. S. W. Tsai, Ed. *Composite Design*, 4th ed. (Think Composites, Dayton, Ohio, 1988), Section 6.
15. P. K. Mallick, *Fiber-Reinforced Composites* (Marcel Dekker, Inc., New York, 1988), Chap. 3.
16. Sunkyong Fiber Co. Ltd., Seoul, Korea.
17. C. Gabriel, E. Isaac, A. Jacob and L. Liviu, *Random Vibration and Reliability of Composite Structures* (Technomic Publishing Co., Inc., Pennsylvania, 1992), Chap. 1 and Chap. 2.
18. Hysol Aerospace and Industrial Products Division, DEXTER Co., Pittsburg, CA, U.S.A.
19. R. S. Alwar and Y. R. Nagaraja, "Viscoelastic analysis of an adhesive tubular joint," *J. Adhesion* **8**, 79–92 (1976).
20. P. J. Hipol, "Analysis of optimization of a tubular lap joint subjected to torsion," *J. Composite Mater.* **18**, 298–311 (1984).
21. M. Imanaka, W. Kishimoto, K. Okita, H. Nakayama and M. Shirato, "Improvement of fatigue strength of adhesive joints through filler addition," *J. Composite Mater.* **18**, 412–419 (1984).
22. D. G. Lee, K. S. Kim and Y. T. Im, "An experimental study of fatigue strength for adhesively bonded tubular single lap joint," *J. Adhesion* **35**, 39–53 (1991).
23. F. L. Matthews, *Joining Fiber-Reinforced Plastics* (Elsevier Applied Science, London and New York, 1986), Chap. 5.
24. S. R. Graves and R. D. Adams, "Analysis of a bonded joint in a composite tube subjected to torsion," *J. Composite Mater.* **15**, 211–224 (1981).
25. F. B. Hildebrand, *Advanced Calculus for Applications*, 2nd ed. (Prentice-Hall, Inc., New Jersey, 1976).
26. MTS Instruments, Minneapolis, Minnesota, U.S.A.
27. Harmonic Drive Ltd., Data sheet and technical manuals (Harmonic drive information service, Seoul, Korea, 1990).